

Internal Motions in a Fulleropyrrolidine Tertiary Amide with Axial Chirality

Giuseppe Borsato,[†] Federico Della Negra,[‡]
 Francesco Gasparrini,[§] Domenico Misiti,[§]
 Vittorio Lucchini,^{*,†} Giorgia Possamai,[‡]
 Claudio Villani,^{*,§} and Alfonso Zambon[†]

*Dipartimento di Studi di Chimica e Tecnologia delle
 Sostanze Biologicamente Attive, Università di Roma "La
 Sapienza", P. le A. Moro 5, 00185 Roma, Italy, Dipartimento
 di Scienze Ambientali, Università di Venezia "Ca' Foscari",
 Dorsoduro 2137, 30121 Venezia, Italy, and Dipartimento di
 Chimica Organica, Università di Padova, Via Marzolo 1,
 35131 Padova, Italy*

claudio.villani@uniroma1.it; lucchini@unive.it

Received March 30, 2004

Abstract: The kinetic parameters for topomerization around the N–CO bond and enantiomerization around the C–CO bond in N-1-naphthoyl fulleropyrrolidine **1** and N-1-naphthoyl pyrrolidine **2** have been determined by dynamic NMR (line shape simulation and selective inversion transfer). The ΔS^\ddagger values are negligible. The ΔH^\ddagger value for topomerization of **1** is smaller with respect to that of **2** by 4.3 kcal mol⁻¹ (explained by the electron-withdrawing effect of fullerene) and the value for enantiomerization is greater by 1.4 kcal mol⁻¹ (explained by the greater rigidity of the fulleropyrrolidine ring, as confirmed by ab initio analyses).

Molecular systems with mechanical properties related to thermal rotation of single bonds have direct implications in the design of miniaturized machinelike components.¹ One functional group whose rotational features and geometric constraints have been studied extensively is the amide fragment, in view of the key role that amide units play in controlling the structure and dynamics of proteins and enzymes.² Tertiary amides with aromatic fragments on the carbonyl side have recently found application as simple molecular devices for the transmission of stereochemical information.³

Here we present our results on the internal dynamics of the axially chiral fulleropyrrolidine amide derivative **1**, a C₆₀ derivative having an N-1-naphthoyl pyrrolidine ring fused to the fullerene spheroid through a 6,6 junction and carrying the amidic rotatable fragment in close proximity of the fullerene surface (Scheme 1).

Tertiary amides of 1-naphthoic acid are known to adopt a conformation in which the naphthyl and the carboxamide planes do not reach a coplanar conformation. This relative disposition of the two fragments renders the molecules chiral and, depending on the substitution pattern of the naphthyl ring and on the size of the nitrogen substituents, the corresponding conformational enantiomers show different interconversion rates in solution.⁴ Rotation around the N–CO axis in the same molecules gives rise to topomerization (the identity reaction leading to exchange of the positions of identical ligands on nitrogen) or diastereoisomerization processes, depending on the symmetry of the parent secondary amine.

Axially chiral fulleropyrrolidine **1** can be considered a simplified model of a prolyl peptide, featuring an unbiased N–CO rotational equilibrium and chirality transferred from the α carbon to the C–CO axis, and as such is especially intriguing in light of the relevance that the motional behavior of acylated proline residues plays in the folding process of proteins.⁵ The effect of the fullerene system on the internal dynamics of **1** is studied here by a combination of dynamic chromatographic and spectroscopic techniques.⁶

Naphthoyl fulleropyrrolidine **1** was prepared by room-temperature acylation of the corresponding NH-fulleropyrrolidine **Fp**, with 1-naphthoyl chloride. The synthesis of **Fp** was carried out starting from the cycloaddition to C₆₀ of the azomethine ylide that forms when glycine and paraformaldehyde are heated at reflux temperature in toluene.⁷ Due to its known lability in the solid state, amine **Fp** was not isolated but directly used in solution, after chromatographic purification, for the acylation step. The related naphthoyl pyrrolidine **2**, devoid of the fullerene fragment, was also prepared and studied as a model compound.

The torsion angle ϕ between the naphthyl and amide planes is defined by the atom sequence OCC₁C₂ (oxygen and carbon of carbonyl, C1 and C2 of naphthyl ring). Ab initio molecular calculations⁸ carried out on **1**⁹ led to the localization of two minima, corresponding to the conformers *s-trans-1* and *s-cis-1* reported in Figure 1 and sketched in Scheme 2, with ϕ angles of 117.4° and 64.1°, respectively. The *s-trans-1* is slightly more stable (by 0.1 kcal mol⁻¹). The interconversions between *s-trans-1* and

[†] University of Venezia.

[‡] University of Padova.

[§] University of Rome.

(1) (a) Balzani, V.; Gomez-Lopez, M.; Stoddart, F. J. *Acc. Chem. Res.* **1998**, *31*, 405–414. (b) Sauvage, J. P. *Acc. Chem. Res.* **1998**, *31*, 611–619.

(2) (a) *The Amide Linkage. Structural Significance in Chemistry, Biochemistry, and Materials Science*; Greenberg, A., Breneman, C. M., Liebman, J. F., Eds.; Wiley-VCH: Weinheim, Germany, 2002. (b) Fischer, G. *Chem. Soc. Rev.* **2000**, *29*, 119–127. (c) Taylor, C. M.; Hardé, R.; Edwards, P. J. B.; Park, J. H. *Org. Lett.* **2003**, *5*, 4413–4416. (d) Shi, T.; Spain, S. M.; Rabenstein, D. L. *J. Am. Chem. Soc.* **2004**, *126*, 790–796.

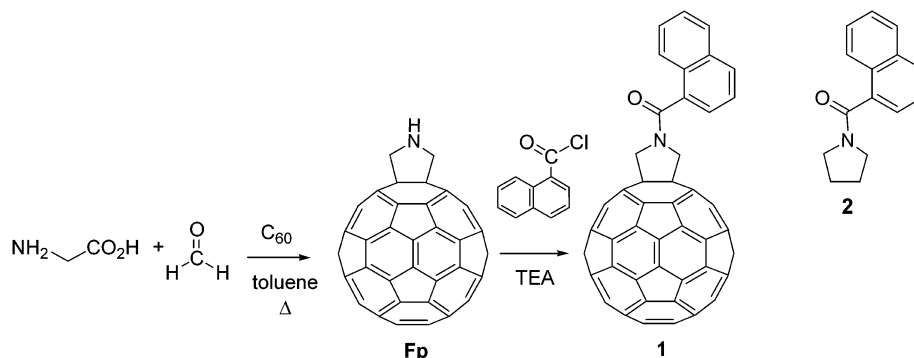
(3) (a) Clayden, J. *Chem. Commun.* **2004**, 127–135. (b) Clayden, J.; Westlund, N.; Frampton, C. S. *J. Chem. Soc., Perkin Trans. 1* **2000**, 1379–1385. (c) Clayden, J.; Pink, J. H.; Yasin, S. A. *Tetrahedron Lett.* **1998**, *39*, 105–108.

(4) (a) Bragg, R. A.; Clayden, J.; Morris, G. A.; Pink, J. H. *Chem. Eur. J.* **2002**, *8*, 1279–1289. (b) Clayden, J.; Pink, J. H. *Angew. Chem.* **1998**, *110*, 2040–2042; *Angew. Chem., Int. Ed.* **1998**, *37*, 1937–1939. (c) Gasparrini, F.; D'Acquarica, I.; Pierini, M.; Villani, C. *J. Sep. Sci.* **2001**, *24*, 941–946. (d) Johnston, E. R.; Fortt, J.; Barborak, J. C. *Magn. Res. Chem.* **2000**, *38*, 932–936. (e) Gasparrini, F.; Misiti, D.; Pierini, M.; Villani, C. *Tetrahedron: Asymmetry* **1997**, *8*, 2069–2073. (f) Pirkle, W. H.; Welch, C. J.; Zych, A. J. *J. Chromatogr. A* **1993**, *648*, 101–109. (g) Cuyekeng, M. A.; Mannschreck, A. *Chem. Ber.* **1987**, *120*, 803–809.

(5) Wedemeyer, W. J.; Welker, E.; Scheraga, H. A. *Biochemistry* **2002**, *41*, 14637–14644.

(6) (a) Zhang, S.; Gan, L.; Huang, C.; Lu, M.; Pan, J.; He, X. *J. Org. Chem.* **2002**, *67*, 883–891. (b) Irngartinger, H.; Weber, A.; Escher, T.; Fettel, P. W.; Gassner, F. *Eur. J. Org. Chem.* **1999**, 2087–2092. (c) Bianco, A.; Lucchini, V.; Maggini, M.; Prato, M.; Scorrano, G.; Toniolo, C. *J. Peptide Sci.* **1998**, *4*, 364–368.

(7) (a) Prato, M.; Maggini, M. *Acc. Chem. Res.* **1998**, *31*, 519–526. (b) Maggini, M.; Scorrano, G.; Prato, M. *J. Am. Chem. Soc.* **1993**, *115*, 9789–9799.

SCHEME 1. Structures of Axially Chiral Amides **1** and **2**, and Synthetic Pathway to **1**

s-cis-1 and between their enantiomers occur through the transition states TS characterized by the ϕ angles shown in Scheme 2.

The calculated electronic energies for TS($\phi = 97.1^\circ$) and TS($\phi = 180^\circ$) are 0.4 and 10.5 kcal mol⁻¹ (with reference to *s-trans-1*). TS($\phi = 180^\circ$) is a *C_s* structure, with a planar pyrrolidine ring coplanar with the CO group, and therefore a true transition state for enantiomerization. The search for TS($\phi = 0^\circ$) is more arduous: the constraint $\phi = 0^\circ$ delivers a structure where the fulleropyrrolidine moiety is pushed away from the naphthalene plane by the steric repulsion between the hydrogen at C₈ and one methylene of the pyrrolidine ring. The energy of this structure is 11.5 kcal mol⁻¹ above that of *s-trans-1*, and that of the true transition state must be even higher. Thus the enantiomer interconversion will occur via TS($\phi = 180^\circ$). The computed barrier is compatible for the monitoring of the enantiomerization process on the NMR time scale, and even for the physical separation of the enantiomers of **1**.

The separation was attempted by low-temperature HPLC on chiral stationary phases. However, using standard analytical columns packed with brush-type chiral packings, we were not able to reach a temperature low enough to freeze or at least to slow the on-column enantiomerization process. On the other hand, the use of a short column packed with 3.5 μ m silica-bonded chiral phase resulted in an almost complete enantioresolution of **1** at -70°C .¹⁰ As the column temperature was raised in 5°C increments, the two chromatographic peaks

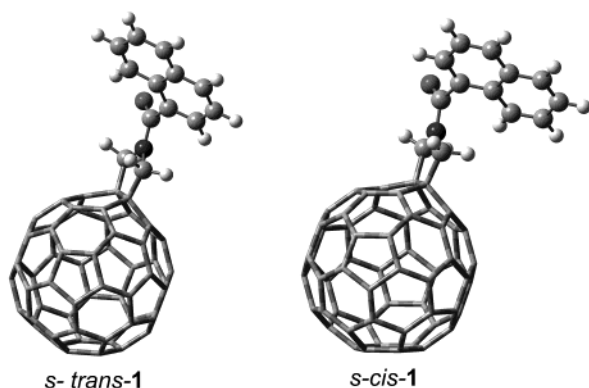
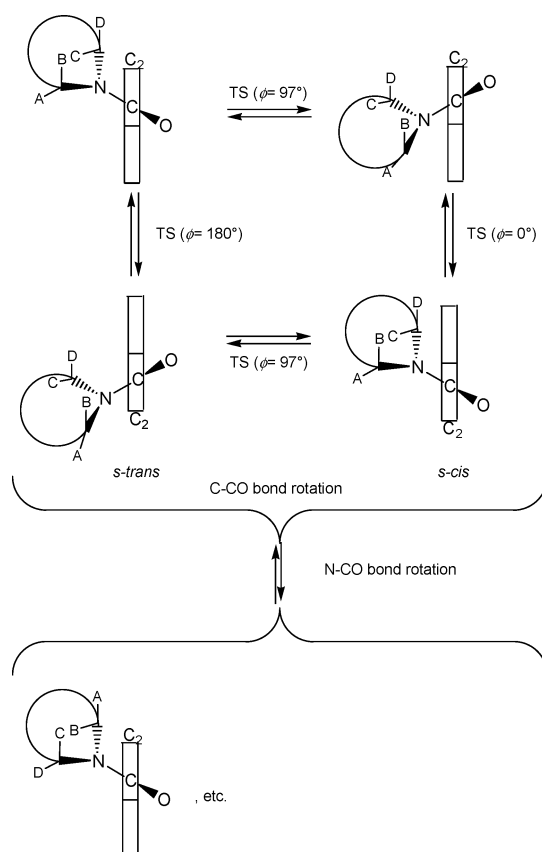
SCHEME 2. Schematic Representations of the Enantiomers and Topomers of the *s-cis* and *s-trans* Conformers of N-1-Naphthoyl Fulleropyrrolidine **1** and N-1-Naphthoyl Pyrrolidine **2** and of Their Interconversion Paths

FIGURE 1. Low-energy structures of the conformers *s-trans-1* and *s-cis-1*, obtained by the ab initio ONIOM implementation: semiempirical PM3 method for the fullerene spheroid, ab initio HF/631G*//631G* for the remnant.

gradually broadened and a plateau appeared between the resolved peaks, indicating accelerated on-column interconversion of the two enantiomers. At -40°C a complete peak coalescence due to fast exchange was observed. Computer simulation of the exchange-broadened elution profiles at -70°C (Figure 2) gave the averaged apparent rate constant for the enantiomer interconversion (C-CO bond rotation) and the corresponding energy barrier $\Delta G^\ddagger = 14.3 \pm 0.2$ kcal mol⁻¹.^{11,12}

A parallel investigation of the internal motions of **1** was carried out by dynamic ¹H NMR. The two methylenes at the 2 and 5 positions of the fused pyrrolidine ring are nonequivalent with N-CO rotation slow on the NMR time scale, while the protons within each methylenic

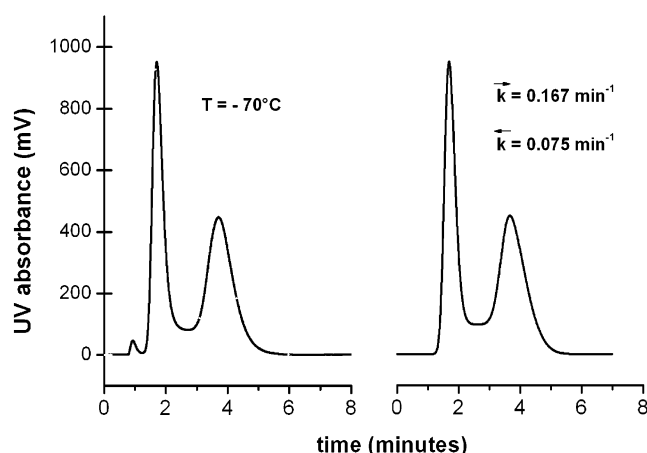


FIGURE 2. Experimental (left) and computer-simulated (right) dynamic HPLC traces for **1**. Experimental chromatogram: column, (*R,R*)-DACH-DNB, 5 cm × 0.40 cm; *T* = −70 °C; eluent, CH₂Cl₂/MeOH 98/2; flow rate, 2.0 mL min^{−1}; UV detection at 280 nm. Simulated chromatogram: *t*₁ = 1.70 min, *t*₂ = 3.77 min, *N*₁ = 68, *N*₂ = 81.

unit are diastereotopic with slow C–CO rotation. Both processes are slow at −35 °C, so that the ¹H NMR (400 MHz) spectrum of **1** (2% w/v in CDCl₃) shows two distinct AB-type subspectra due to the hydrogens labeled (AB) and (CD) in Scheme 2. As the temperature was raised the lines within each AB set progressively broaden and eventually coalesce at about 0 °C, leaving two broad lines for each methylene unit. These temperature-dependent spectral changes are consistent with C–CO bond rotation becoming increasingly faster on the NMR time scale (enantiomerization process). The line shape simulation¹³ was carried out on the signals of the low-field AB subspectrum, which displays more separated doublets (see the Supporting Information). Fitting of the obtained rate constants into the Eyring equation gave the activation parameters (reported in Table 1) for the enantio-

TABLE 1. Kinetic Parameters for Enantiomerization around the C–CO Bond and Topomerization around the N–CO Bond in *N*-1-Naphthoyl Fulleropyrrolidine **1** and *N*-1-Naphthoyl Pyrrolidine **2**

compd	bond rotation	points	temp range, °C	ΔH^\ddagger , kcal mol ^{−1}	ΔS^\ddagger , cal mol ^{−1} K ^{−1}
1	C–CO	15 ^a	−22.5 to 15.0	13.5 ± 0.1	−0.4 ± 0.1
	N–CO	12 ^a	10.0 to 65.0	16.0 ± 0.1	−0.4 ± 0.1
2	C–CO	22 ^a	−57.5 to 0.0	12.1 ± 0.1	1.7 ± 0.1
	N–CO	7 ^b	40.0 to 65.0	20.3 ± 0.2	4.1 ± 0.1

^a By ¹H NMR line-shape analysis. ^b By ¹H NMR selective inversion recovery.

meric interconversion of **1**. Simple steric considerations and the results of the ab initio investigation will suggest that the observed enantiomerization actually occurs through the transition state TS(ϕ = 180°). The energy barrier determined by NMR is very similar to the one extracted by HPLC, despite the differences in the solvent systems and temperature ranges for the two experiments, a situation that has been observed in related studies.^{10a}

Further heating of the sample resulted in additional line broadening and partial collapse of the two resonances, a spectral change indicating increasingly faster N–CO bond rotation. The line shape simulations (see the Supporting Information) required the rate constants for the C–CO rotation, whose values were either obtained from the preceding simulation or were extrapolated to higher temperatures. Fitting the rate constants into the Eyring equation gave the activation parameters reported in Table 1.

The ¹H NMR subspectrum (400 MHz) at −65.0 °C of the ring methylenic protons of naphthoyl pyrrolidine **2** (2% w/v in CDCl₃) displays 4 complicated multiplets, which, however, simplify to 2 quintets (3 and 4 positions) and to 2 triplets (2 and 5 positions) already at 0 °C. Thus, both the C–CO and the N–CO rotations are “frozen” at low temperature, and the above process describes increasingly fast rotation around the C–CO bond. Because of the greatest separation of the resonances of the diastereotopic protons, the temperature-dependent broadening, collapse, and resharping of the lines into a final triplet are most clearly evident in the multiplet resonating at δ 3.14. This multiplet was therefore subjected to line shape simulation (see the Supporting Information).¹³ The fitting into the Eyring equation gave the activation parameters for the enantiomeric interconversion of **2** reported in Table 1.

The subspectrum of **2** featuring 2 triplets and 2 quintets remains unaltered in the temperature range between 0 and 60 °C, a situation consistent with N–CO bond rotation always being slow on the NMR time scale. Rate constants for this process were obtained by selective inversion transfer experiments.¹⁴ The low-field triplet of one methylene unit α to pyrrolidine nitrogen was selectively inverted by a soft shaped pulse and a series of spectra were acquired with increasing delays (from 0.06 to 1.2 s) between the soft and the hard pulses. The residual magnetization in the *x*–*y* plane, caused by incomplete inversion, was suppressed by a 180° shift of the transmitter phase every second transient in a four-transient run. The *z*-magnetization was clearly trans-

(8) Frisch, M. J.; Trucks, G. W.; Schlegel, H. B.; Scuseria, G. E.; Robb, M. A.; Cheeseman, J. R.; Zakrzewski, V. G.; Montgomery, J. A., Jr.; Stratmann, R. E.; Burant, J. C.; Dapprich, S.; Millam, J. M.; Daniels, A. D.; Kudin, K. N.; Strain, M. C.; Farkas, O.; Tomasi, J.; Barone, V.; Cossi, M.; Cammi, R.; Mennucci, B.; Pomelli, C.; Adamo, C.; Clifford, S.; Ochterski, J.; Petersson, G. A.; Ayala, P. Y.; Cui, Q.; Morokuma, K.; Malick, D. K.; Rabuck, A. D.; Raghavachari, K.; Foresman, J. B.; Cioslowski, J.; Ortiz, J. V.; Stefanov, B. B.; Liu, G.; Liashenko, A.; Piskorz, P.; Komaromi, I.; Gomperts, R.; Martin, R. L.; Fox, D. J.; Keith, T.; Al-Laham, M. A.; Peng, C. Y.; Nanayakkara, A.; Gonzalez, C.; Challacombe, M.; Gill, P. M. W.; Johnson, B. G.; Chen, W.; Wong, M. W.; Andres, J. L.; Head-Gordon, M.; Replogle, E. S.; Pople, J. A. *Gaussian 98*, revision 5.4; Gaussian, Inc.: Pittsburgh, PA, 1998.

(9) (a) Geometrical optimization by the ONIOM implementation: semiempirical PM3 method for the fullerene spheroid, ab initio HF/631G*/631G* for the remnant. (b) Similar results have been described for *N,N*-dimethyl-1-naphthamide: Campomanes, P.; Menendez, M. I.; Sordo, T. L. *J. Phys. Chem. A* **2002**, *106*, 2623–2628.

(10) Column: 5 × 0.4 cm² packed with (*R,R*)-DACH-DNB chiral stationary phase. Standard analytical columns packed with the same chiral phase are available from Regis Technologies, Morton Grove, IL. (a) Gasparrini, F.; Lunazzi, L.; Mazzanti, A.; Pierini, M.; Pietrusiewicz, K. M.; Villani, C. *J. Am. Chem. Soc.* **2000**, *122*, 4776–4780. (b) Gasparrini, F.; Misiti, D.; Villani, C. *J. Chromatogr. A* **2001**, *906*, 35–50.

(11) Experimental chromatograms were simulated by using a modified version of the SIMUL package.^{4e,11} The simulation procedure yields separated apparent rate constants for the interconversion of the two enantiomers, and the averaged value is used to calculate ΔG^\ddagger .

(12) (a) Jung, M. *QCPE Bull.* **1992**, *12*, 52. (b) Jung, M.; Schurig, V. *J. Am. Chem. Soc.* **1992**, *114*, 529–534.

(13) (a) Stephenson, D. S.; Binsch, G. *J. Magn. Reson.* **1978**, *32*, 145–152. (b) Stephenson, D. S.; Binsch, G. *DNMR5*, *QCPE* 365; modified by LeMaster, C. B.; LeMaster, C. L.; True, N. S. *QCMP* 059.

(14) Alger, J. R.; Prestgard, J. H. *J. Magn. Reson.* **1977**, *27*, 137–141.

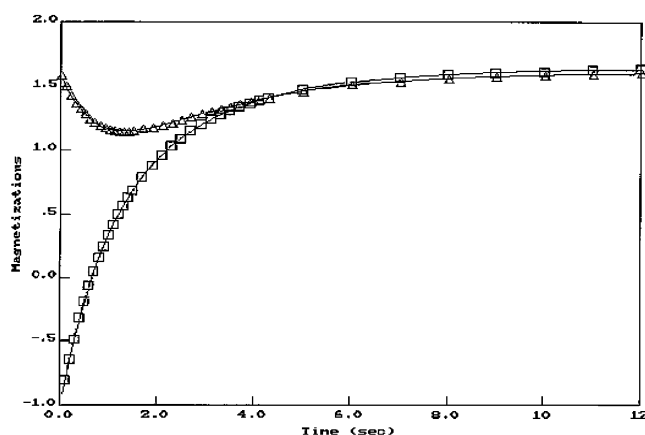


FIGURE 3. Saturation transfer experiment for compound **2**, carried out at 40 °C. The low-field triplet of the pyrrolidine ring (\square) is inverted and the magnetization is transferred to the high-field triplet (\triangle). The data are fitted into the algorithm proposed by ref 14.

ferred to the other α methylene unit, and the delay dependence of the intensity changes for the two signals was fitted into the proper algorithm.¹⁴ One example of fitting is provided in Figure 3. The algorithm gave the rate constants for the magnetization transfer, which are also the constants for the topomerization process. The fitting to the Eyring equation gave the activation parameters (reported in Table 1) for the N–CO rotation in amide **2**.

Customarily, activation entropies smaller than 5 cal mol⁻¹ K⁻¹ are considered about 0, and negligible values of ΔS^\ddagger can then be assumed for N–CO and C–CO bond rotations in **1** and **2**.

While the rotational barrier for the N–CO bond in amide **2** compares well with that of *N*-acylated proline measured in solvents of low polarity,¹⁵ the same barrier is significantly smaller in **1**.

Fast N–CO rotation in **1** can be interpreted in terms of attenuated resonance stabilization of the planar ground state of **1** relative to that of **2**.¹⁶ The C₆₀ fullerene fragment exerts a strong electron-withdrawing effect, as evidenced by the unusually low nitrogen basicity and nucleophilicity measured for a fulleropyrrolidine structurally related to **1**.^{5c,17} The 4.3 kcal mol⁻¹ lowering of the N–CO rotational barrier in **1** compared to the model amide **2** is consistent with a diminished π nitrogen–carbonyl interaction and reduced C–N bond order in the ground state of **1**.

The barrier to C–CO bond rotation in **1** is 1.4 kcal mol⁻¹ larger than that of amide **2**, suggesting that the process is hindered somewhat by some property of the C₆₀ spheroid. Enantiomer interconversion by C–CO rotation requires the passage of the pyrrolidine unit past the less sterically demanding C₂ position of the naphthyl

ring, as described by the transition state TS($\phi = 180^\circ$) in Scheme 2. The small observed effect might be a consequence of the increased rigidity of the pyrrolidine ring when it is fused to the C₆₀ framework, resulting in a more strained transition state. On the contrary, the electron-withdrawing effect of the fullerene should induce a greater conjugation of the carbonyl with the naphthyl ring in the transition state, and therefore a barrier lowering. These hypotheses could be tested by the comparative calculations¹⁸ performed on naphthoyl pyrrolidine **2**, naphthoyl 3-fluoropyrrolidine **3** (which mimics the electron-withdrawing effect of the fullerene spheroid), and naphthoyl pyrroline **4** (which mimics the rigidity of the fulleropyrrolidine ring). The *s-trans* conformer is always the more stable, and the enantiomer interconversion energies through TS($\phi = 180^\circ$) are 9.2, 9.1, and 9.6 kcal mol⁻¹ for **2**, **3**, and **4** respectively. The rigidity of the fulleropyrrolidine ring seems to play the major role.

In summary, placing the fullerene fragment close to the amide nitrogen accelerates amide C–N rotation by a factor of 10³ at room temperature and to some extent retards enantiomerization by C–CO rotation.

The unusually low barrier to N–CO rotation found for **1** may be exploited to prepare larger structures of biological relevance incorporating *N*-acylated fulleropyrrolidine fragments and featuring increased rates of conformational exchange between two or more non-equivalent states.¹⁹

Experimental Section

Synthesis of 1: A solution of 342 mg of C₆₀ (0.48 mmol), 75 mg of glycine (1.0 mmol), and 50 mg of paraformaldehyde (1.67 mmol) in 300 mL of toluene was heated to reflux for 2 h. Then the mixture was concentrated to about half volume, loaded on top of a SiO₂ flash chromatography column, and eluted with toluene to remove unreacted C₆₀, then with toluene/ethyl acetate 95:5. The fractions containing NH-fulleropyrrolidine **Fp** (TLC: toluene/EtOAc 9:1, *R_f* 0.3) were concentrated to ca. 60 mL. To this solution were added triethylamine (100 μ L) and 1-naphthoyl chloride (50 μ L, 0.33 mmol) and the mixture was stirred at room temperature for 30 min (TLC: toluene/EtOAc 9:1, *R_f* 0.6). The solvent was removed in vacuo and the residue washed several times with methanol in a centrifuge tube. Pure fulleropyrrolidine **1** (39 mg) was isolated (9%, based on starting C₆₀). UV–vis (CH₂Cl₂) λ (ϵ (dm³ mol⁻¹ cm⁻¹)) 256 (11640), 310 (36620), 430 (3100) nm; ¹H NMR (250 MHz, CDCl₃/CS₂/TMS) δ 8.38 (d, 1H), 7.88 (m, 4H), 7.62 (m, 4H), 5.80 (br s, 2H), 5.17 (br s, 2H) ppm; ¹³C NMR (62.5 MHz, CDCl₃/CS₂) δ 168.6, 152.5 (br), 147.1, 146.1, 145.9, 145.4, 145.2, 145.1, 144.2, 142.9, 142.8, 142.4, 141.9, 141.8, 141.6, 139.9 (br), 135.6 (br), 133.5, 133.1, 130.2, 129.7, 128.4, 127.3, 126.7, 125.1, 125.0, 124.9, 70.7 (br), 60.6 (br), 56.6 (br) ppm; ESI-MS C₇₃H₁₁ON *m/z* 918 (M + H)⁺. Calcd. elemental analysis for C₇₃H₁₁ON (917): C 95.52; H 1.21; N 1.53. Found: C 94.66; H, 1.15; N 1.49.

Acknowledgment. This work was supported by MIUR (PRIN. 2002, prot. 2002032171).

Supporting Information Available: Experimental and simulated NMR spectra and Eyring plots for **1** and **2** and calculated structures and the corresponding transition states. This material is available free of charge via the Internet at <http://pubs.acs.org>.

JO049485Q

(15) Eberhardt, E. S.; Panasiak, N.; Raines, R. T. *J. Am. Chem. Soc.* **1996**, *118*, 12261–12266.

(16) According to ab initio valence bond calculations, about one-half of the barrier to C–N rotation in amides is due to a π interaction between the amide nitrogen and the carbonyl group: (a) Wiberg, K. B.; Rush, D. J. *J. Am. Chem. Soc.* **2001**, *123*, 2038–2046. (b) Lauvergnat, D.; Hilbert, P. C. *J. Am. Chem. Soc.* **1997**, *119*, 9478–9482.

(17) (a) Bagno, A.; Claeson, S.; Maggini, M.; Martini, M. L.; Prato, M.; Scorrano, G. *Chem. Eur. J.* **2002**, *8*, 1015–1023. (b) D'Souza, F.; Zandler, M. E.; Deviprasad, G. R.; Wutner, W. *J. Phys. Chem. A* **2000**, *104*, 6887–6893.

(18) Ab initio HF/631G**//631G*.

(19) For bioincorporation of fluorine-substituted proline into proteins, see: Renner, C.; Alefelder, S.; Bac, J. H.; Budisa, N.; Huber, R.; Moroder, L. *Angew. Chem., Int. Ed.* **2001**, *40*, 923–925.